Tracking unstable orbits in chaos using dissipative feedback control

N. F. Rulkov* and L. S. Tsimring†
Institute for Nonlinear Science, University of California, San Diego, Mail Code 0402, La Jolla, California 92093-0402

Henry D. I. Abarbanel‡
Department of Physics and Marine Physical Laboratory, Scripps Institution of Oceanography, University of California, San Diego, Mail Code 0402, La Jolla, California 92093-0402

(Received 10 January 1994)

Using a form of linear feedback we call *dissipative feedback control,* we show how to use external forcing to control a chaotic dynamical system to a fixed point or an unstable periodic orbit when the location of the fixed point or unstable periodic orbit may change slowly with time. The ability to follow a desired state of the system by an external control even when that state is slowly varying in time we call *tracking.* This slow "drift" of states is the usual situation in actual experimental realizations of chaotic systems in nonlinear circuits and other physical manifestations, and this drift can be accounted for by providing a slow dynamics for the location of the fixed point or periodic orbit. We discuss the theoretical aspects of this idea and show its feasibility in some experiments with nonlinear circuits with chaotic behavior.

PACS number(s): 47.20.Ky, 47.27.Te, 64.90.+b

I. INTRODUCTION

In the investigation of means of controlling chaotic dynamical systems many suggestions have been made [1–4] which employ different strategies for effecting the control. The method of Ott, Grebogi, and Yorke [1] focuses on the variation of an accessible parameter of the dynamical system to stabilize the motion to one of the unstable fixed points or unstable periodic orbits which abound within the strange attractor visited by the chaotic orbit. If system noise is small, then the main advantage of the parameter variation method is that using essentially any accessible parameter one may move the orbits to one of these formerly unstable orbitals with very small perturbations and can achieve this without knowledge of the governing equations of the system. A disadvantage of the method is that it requires that the small perturbations be computed at each step and thus the control becomes infeasible for high frequency motions. Of course, since the method requires the use of the local stable and unstable manifolds of the unstable fixed point or periodic orbit, noise can drive one away from the convenient operating region and break the control. Further, if the local Lyapunov exponents of the system being controlled are large, the ability to achieve control with only small perturbations may be jeopardized.

In this paper we investigate a somewhat different approach to control based on *variation of one or a few of the dynamical variables* of the system in an appropriate way. This method in application to the stabilization of unstable periodic orbits of chaotic dynamical systems was first suggested and illustrated numerically by Pyragas [4]. We call this principle "dissipative feedback control" and will illustrate it below. The general technique has been used in control theory for some years and is known as "closed-loop state feedback control" [5]. The central idea is to measure some physical dynamical variable $\mathbf{x}(t)$ and then find a way to drive $\mathbf{x}(t)$ towards the desired value $\mathbf{x}_D(t)$ by adding a term proportional to $\mathbf{x}(t)-\mathbf{x}_D(t)$ in the equations of motion for $\mathbf{x}(t)$ in such a way that the motion "dissipatively" moves $\mathbf{x}(t)\rightarrow\mathbf{x}_D(t)$. If $\mathbf{x}_D(t)$ is an existing but unstable orbit of the initial dynamical system, then, after an initial transient, stabilization to this now stable orbit can be achieved with very small "energy expenditure" required in the control process. Even if $\mathbf{x}_D(t)$ does not correspond to a stationary state of the system, stabilization still can be achieved, but with finite energy losses. To a certain extent, this method is similar to the method of occasional proportional feedback control which was employed for stabilizing periodic orbits [3] and recently for synchronization of chaotic circuits [6]. The main advantage of this scheme is in its simplicity—one can provide control without computing parameter perturbations and by using analog hardware only. Another advantage is that this method can in principle provide global stability and therefore be much less sensitive to noise than the parameter perturbation techniques. Although it may seem difficult to find an appropriate way to introduce dissipative feedback into the unknown system, we envision a large number of situations when this is possible. For example, in a thermofluid setting, if one measures temperature variations, then the heat supply to the location of measurements would provide a natural dissipative feedback. Dissipative feedback to light intensity in chaotic laser experiments can be achieved by varying the quality factor Q of the resonator. Of course, when one works with chaotic electronic circuits, the dissipative coupling is usually quite easy to implement as a current injected through a resistive coupling. Finally, in

*Electronic address: rulkov@hamilton.ucsd.edu
†Electronic address: lev@legendre.ucsd.edu
‡Also at Institute for Nonlinear Science; electronic address: hdia@hamilton.ucsd.edu

controlling fluid turbulence in a boundary layer on spatial scales where coherent structures are the dominant dynamics [7], control would be established by a pressure feedback of the sort discussed here.

The goal of this paper is to demonstrate how one can use the method of dissipative feedback for tracking unstable fixed points and unstable periodic orbits throughout the chaotic domain of the bifurcation diagram for a system. We suggest an algorithm with which one can start control at the value of control parameter when the fixed point or periodic orbit is stable, and then as one slowly changes a control parameter and enters a chaotic state through a sequence of bifurcation still have the system remain near the selected but now unstable periodic orbit or fixed point. Unlike tracking schemes using parameter control [8], it is not necessary to know the eigenvalues and eigenvectors of the unstable fixed point or periodic orbit throughout the range of parameter variation. In most cases it is only necessary to choose the sign of one or a few parameters appropriately.

In Sec. II we will present a general formulation of the method and discuss when dissipative feedback tracking will work. In Sec. III we will consider an important particular case when a chaotic system can be controlled by a scalar dissipative feedback. In Sec. IV we will present results from actual experiments with the electronic circuit illustrating possibility of tracking an unstable fixed point using dissipative feedback control. The last section contains our conclusions.

II. GENERAL FORMULATION

A. Fixed points

We begin with a dynamical system

$$\frac{d\mathbf{x}(t)}{dt}=\mathbf{F}(\mathbf{x}(t)) , \tag{1}$$

where $\mathbf{F}(\ )$ is a vector valued function of $\mathbf{x}=(x_1,x_2,\ldots,x_d)$ in d dimensions. The dissipative feedback control scheme can be expressed in the following form:

$$\frac{d\mathbf{x}(t)}{dt}=\mathbf{F}(\mathbf{x}(t))+\mathbf{g}[\mathbf{x}_D(t)-\mathbf{x}(t)] . \tag{2}$$

Here $\mathbf{x}_D(t)$ is a given stable or unstable periodic orbit or fixed point of the original system (1). $\mathbf{x}_D(t)$ is the desired state of the system to which we wish to drive it by our additional control. $\mathbf{g}$ is a $d\times d$ diagonal matrix with elements $\mathbf{g}_{ij}=g_i\delta_{ij};g_i\geq 0;i,j=1,2,\ldots,d$. It is easy to see that for any dynamical system (1) one can find a $g_0>0$ such that, if all $g_i>g_0$, the trajectory $\mathbf{x}_D(t)$ becomes stable. This simply says that if one drives the orbit strongly enough in a dissipative fashion near $x_D(T)$, it will go there stably. Although the g_0 accomplishing this goal is not small in general, as it is of the order of the largest Lyapunov exponent of the particular unstable periodic orbit $\mathbf{x}_D(t)$, the driving becomes in fact arbitrarily small as soon as the system approaches the chosen orbit, since we then have $\mathbf{g}[\mathbf{x}_D(t)-\mathbf{x}(t)]\rightarrow 0$.

This control method is generic in the sense that all control schemes change the dynamical system with which one works by adding an "external" forcing to the system designed to drive the augmented system to a specified location in state space. In our examples we have chosen to drive the original system to a "desired state" $\mathbf{x}_D(t)$ which was an unstable state of the original system. We do this because the unstable fixed points and unstable periodic orbits of the dynamics $d\mathbf{x}(t)/dt=\mathbf{F}(\mathbf{x}(t))$ are characteristic of the system [9] and there are methods for establishing these without knowledge of $\mathbf{F}(\ )$ from observed orbits $\mathbf{x}(t)$ alone.

In many physically interesting cases dissipation can only be applied to one or a few components of the vector $\mathbf{x}(t)$ of dynamical variables. This means only a few entries of $\mathbf{g}$ are nonzero. In order to stabilize the familiar Lorenz system, for example, only the x component may be "dissipated," as the other subsystems arising when one tries to dissipate either the y or z components of the Lorenz system are unstable. Usually the number of dynamical variables to be controlled by dissipation coincides with the number of positive Lyapunov exponents in the uncontrolled system. In some cases it can be fewer. The particular choice of dynamical variables to which the dissipative feedback should be applied is not always obvious, although physical intuition can often help to choose the "most unstable" variables. The sufficient condition for the right choice is that the equation for the remaining variables form a stable subsystem with all negative conditional Lyapunov exponents [10] (see Sec. III for more details). For noisy systems the driving magnitude remains finite, as in the parameter control schemes; however, in the present method we can be sure that fairly large fluctuations do not throw the system out of control for an indefinitely long time. For example, if g_0 is larger than the largest Lyapunov exponent of the uncontrolled chaotic attractor, the orbit we chose with $\mathbf{x}_D(t)$ becomes a global attractor.

From now on we will concentrate on the case when the desired orbit $\mathbf{x}_D(t)=\mathbf{x}^*$ which is an unstable fixed point of the original system, $\mathbf{F}(\mathbf{x}^*)=\mathbf{0}$. In real experiments the exact position of the desired fixed point is usually unknown, especially if the parameters of the system vary slowly in time. In this case we can generalize the dissipative feedback control scheme (2) by allowing the value of $\mathbf{x}_D$ to change slowly under the influence of the system:

$$\frac{d\mathbf{x}(t)}{dt}=\mathbf{F}(\mathbf{x}(t))+\mathbf{g}[\mathbf{x}_D(t)-\mathbf{x}(t)] , \tag{3}$$

$$\frac{d\mathbf{x}_D(t)}{dt}=\mu\beta[\mathbf{x}(t)-\mathbf{x}_D(t)] , \tag{4}$$

where $\mu\ll 1$, and β is a $d\times d$ matrix to be specified. The particular choice of β depends on the properties of the unstable fixed point we will try to stabilize. The idea here is that the system goes to the surface $\mathbf{F}(\mathbf{x})+\mathbf{g}(\mathbf{x}_D-\mathbf{x})=0$ on a rapid time scale which is of order unity, and then on a time scale of order μ^{-1} adjusts the value of $\mathbf{x}_D$ so that $\mathbf{x}(t),\mathbf{x}_D(t)\rightarrow\mathbf{x}^*;\mathbf{F}(\mathbf{x}^*)=0$.

With the small parameter μ the system (3) and (4) exhibits motions on two time scales as noted. In the limit $\mu\rightarrow 0$ the hypersurface on which slow motion, that is, the

variation of $\mathbf{x}_D(t)$, occurs is described by

$$\mathbf{F}(\mathbf{x})=\mathbf{g}(\mathbf{x}-\mathbf{x}_D)\ , \tag{5}$$

and the fast motion is along the one parameter family of hyperplanes $\mathbf{x}_D=\text{const}$. Fixed points of the original system (1) lie on intersections of the surface of slow motion and the surface $\mathbf{x}=\mathbf{x}_D$. Following Eq. (3) brings $\mathbf{x}$ onto a surface of slow motion (5) with $\mathbf{x}_D=\mathbf{x}_D(0)$. During the subsequent slow evolution $\mathbf{x}$ and $\mathbf{x}_D$ change, preserving the relation (5) and in accordance with Eq. (4). To assure that $\mathbf{x}_D$ moves towards the fixed point $\mathbf{x}^*$ of the original system one needs to make a special choice of the matrix β. Near the fixed point $\mathbf{x}=\mathbf{x}_D=\mathbf{x}^*$ we can take a local linear approximation for $\mathbf{F}(\mathbf{x})$,

$$\begin{aligned}\mathbf{F}(\mathbf{x})&=\mathbf{F}(\mathbf{x}^*)+\mathbf{DF}(\mathbf{x}^*)(\mathbf{x}-\mathbf{x}^*)\\&=\mathbf{DF}(\mathbf{x}^*)(\mathbf{x}-\mathbf{x}^*)\end{aligned} \tag{6}$$

[$\mathbf{DF}(\mathbf{x}^*)$ is the $d\times d$ Jacobian matrix of the original system evaluated at the fixed point $\mathbf{x}^*$] and rewrite (5) as

$$\begin{aligned}\mathbf{DF}(\mathbf{x}^*)(\mathbf{x}-\mathbf{x}^*)&=\mathbf{g}(\mathbf{x}-\mathbf{x}_D)\\&=\mathbf{g}[(\mathbf{x}-\mathbf{x}^*)-(\mathbf{x}_D-\mathbf{x}^*)]\end{aligned} \tag{7}$$

or

$$\mathbf{x}-\mathbf{x}^*=-[\mathbf{DF}(\mathbf{x}^*)-\mathbf{g}]^{-1}\mathbf{g}(\mathbf{x}_D-\mathbf{x}^*)\ . \tag{8}$$

We are assuming that the matrix $\mathbf{DF}(\mathbf{x}^*)-\mathbf{g}$ is nonsingular and all its eigenvalues are negative. All of this gives an equation for $\mathbf{x}_D(t)-\mathbf{x}^*$:

$$\frac{d[\mathbf{x}_D(t)-\mathbf{x}^*]}{dt}=-\mu\beta[(\mathbf{DF}-\mathbf{g})^{-1}\mathbf{g}+\mathbf{I}][\mathbf{x}_D(t)-\mathbf{x}^*]\ . \tag{9}$$

Now suppose $\mathbf{C}$ is a unitary matrix such that $\mathbf{A}=\mathbf{C}[(\mathbf{DF}-\mathbf{g})^{-1}\mathbf{g}+\mathbf{I}]\mathbf{C}^{-1}$ is triangular. If all diagonal elements A_{ii} of $\mathbf{A}$ are nonzero, we can choose

$$\beta=\mathbf{C}^{-1}\mathbf{G}\mathbf{C}\ , \tag{10}$$

where $\mathbf{G}$ is, for example, a diagonal matrix with elements $G_{ii}=-\text{sgn}A_{ii}$). Then all eigenvalues of the system (9) will be negative:

$$\lambda_i=-|A_{ii}|\ . \tag{11}$$

If $\mathbf{A}$ is singular, we can always add nondiagonal parts to $\mathbf{G}$ to make the corresponding eigenvalues of (9) negative.

In the general formulation presented here the technique of dissipative feedback control may appear not easier to implement than parameter variation methods. However, in many cases the general procedure may be greatly simplified. Indeed, if the system can be separated into "active" and "stable" subsystems, the dissipative feedback need only be applied to the "active" dynamical variables. Once these variables are determined (which often can be done purely on experimental grounds), the dissipative feedback can actually be provided without knowledge of the underlying dynamical equations of motion. In Sec. III we consider a particularly simple case when the system has just one "active" variable and can be stabilized by a scalar dissipative feedback.

B. Unstable periodic orbits

If we wish to stabilize an unstable periodic orbit of the system, we apply the method just outlined to a sequence of Poincaré sections. On these Poincaré sections the flow becomes a discrete time map with the "time" label n indicating the sequence of crossings of the section. The vectors in the section are $(d-1)$-dimensional $\mathbf{x}(n);n=1,2,\ldots,N$. From the flow we make the finite time map

$$\mathbf{x}(n+1)=\mathbf{x}(n)+\mathbf{f}(\mathbf{x}(n))\ , \tag{12}$$

and with dissipative feedback control this becomes

$$\mathbf{x}(n+1)=\mathbf{x}(n)+\mathbf{f}(\mathbf{x}(n))+\mathbf{g}[\mathbf{x}_D(n)-\mathbf{x}(n)]\ . \tag{13}$$

As above we are seeking a fixed point in the Poincaré section at $\mathbf{x}^*$ with $\mathbf{f}(\mathbf{x}^*)=\mathbf{0}$.

We would, in practice, seek to move the orbit in a sequence of sections $\mathbf{x}_a(n)$ to a sequence of fixed points $\mathbf{x}_a^*$. The spacing of the sequence of sections must be chosen so that the features of the unstable periodic orbit which crosses the sections at the points $\mathbf{x}_a^*$ are properly captured. To assure this we should place the sections within a half wavelength or less of each variation about the orbit. Where the orbit is smooth, fewer sections are required. Where the orbit has substantial curvature, more sections will be needed. On each section we perform the operations now to be described for a given section.

First we augment the dissipative feedback evolution with an equation operating on a slow time scale for the variation of $\mathbf{x}_D$:

$$\mathbf{x}_D(n+1)=\mathbf{x}_D(n)+\mu\beta[\mathbf{x}(n)-\mathbf{x}_D(n)] \tag{14}$$

as above; $\mu\ll 1$, so there are again slow motions governed by this last equation and rapid motions governed by the original dynamics. The orbits $\mathbf{x}(n)$ rapidly move onto the hyper surface

$$\mathbf{f}(\mathbf{x}(n))+\mathbf{g}[\mathbf{x}_D(n)-\mathbf{x}(n)]=0\ . \tag{15}$$

Assuming we start near the fixed point $\mathbf{x}^*$, we can write

$$\mathbf{f}(\mathbf{x})=\mathbf{f}(\mathbf{x}^*)+\mathbf{Df}(\mathbf{x}^*)(\mathbf{x}-\mathbf{x}^*)\ , \tag{16}$$

and note $\mathbf{f}(\mathbf{x}^*)=\mathbf{0}$. Following the development above we write

$$\begin{aligned}[\mathbf{x}(n)-\mathbf{x}^*]\mathbf{Df}(\mathbf{x}^*)&=\mathbf{g}[\mathbf{x}(n)-\mathbf{x}_D(n)]\\&=\mathbf{g}[\mathbf{x}(n)-\mathbf{x}^*]+\mathbf{g}[\mathbf{x}^*-\mathbf{x}_D(n)]\end{aligned} \tag{17}$$

or

$$[\mathbf{Df}(\mathbf{x}^*)-\mathbf{g}][\mathbf{x}(n)-\mathbf{x}^*]=-\mathbf{g}[\mathbf{x}_D(n)-\mathbf{x}^*]\ . \tag{18}$$

Using this relation in the slow evolution equation for $\mathbf{x}_D(n)$,

$$\mathbf{x}_D(n+1)=\mathbf{x}_D(n)+\mu\beta[\mathbf{x}(n)-\mathbf{x}_D(n)]\ , \tag{19}$$

we arrive at

$$\begin{aligned}\mathbf{x}_D(n+1)-\mathbf{x}^*&=\mathbf{x}_D(n)-\mathbf{x}^*+\mu\beta[\mathbf{x}(n)-\mathbf{x}^*+\mathbf{x}^*-\mathbf{x}_D(n)]\\&=\mathbf{x}_D(n)-\mathbf{x}^*-\mu\beta\{\mathbf{x}_D(n)-\mathbf{x}^*+[\mathbf{Df}(\mathbf{x}^*)-\mathbf{g}]^{-1}\mathbf{g}[\mathbf{x}_D(n)-\mathbf{x}^*]\}\\&=[\mathbf{I}+\mathbf{M}][\mathbf{x}_D(n)-\mathbf{x}^*]\ ,\end{aligned} \tag{20}$$

with

$$\mathbf{M}=-\mu\beta\{\mathbf{I}+[\mathbf{Df}(\mathbf{x}^*)-\mathbf{g}]^{-1}\mathbf{g}\}\ . \tag{21}$$

The stability of the approach $\mathbf{x}_D(n)\to\mathbf{x}^*$ is determined by the eigenvalues of the matrix $\mathbf{M}$ as before.

So the extension of the methods outlined above for moving a system to a fixed point and allowing the control algorithm to adjust to slow variations in the location of the fixed point can be extended to controlling the orbits of the chaotic system to periodic orbits by making adjustments along the orbit in a sequence of Poincaré sections.

III. SCALAR TRACKING OF UNSTABLE FIXED POINTS

In this section we separate the dynamical system (1) into an equation for an "active" *scalar* dynamical variable $x(t)$ and $d-1$ equations for the rest of the dynamical variables $\mathbf{y}(t)$. The $\mathbf{y}(t)$ are taken to be a stable subsystem. The evolution equations then split into the pair

$$\begin{aligned}\frac{dx(t)}{dt}&=h(x(t),\mathbf{y}(t))\ ,\\ \frac{d\mathbf{y}(t)}{dt}&=\mathbf{S}(x(t),\mathbf{y}(t))\ .\end{aligned} \tag{22}$$

The stability of the subsystem $\mathbf{y}(t)$ for a given trajectory $\{x(t),\mathbf{y}(t)\}$ is determined by the conditional Lyapunov exponents [10] which are calculated by iterating the "partial" Jacobian $\mathbf{DS}(x(t),\mathbf{y}(t))=\{\partial S_i(x(t),\mathbf{y}(t))/\partial y_j\}$ along that orbit. When all these exponents λ_a, $a=1,2,\ldots,d-1$, are negative, $\mathbf{y}(t)$ is said to form the *stable subsystem* [10]. We note in passing that this stability can be local (near a particular orbit or a fixed point), or global if conditional Lyapunov exponents are negative for any orbit of the system.

Now we assume that $\mathbf{y}(t)$ forms a stable subsystem near the unstable fixed point. It is easy to see then that the scalar dissipative feedback control for the dynamical variable $x(t)$

$$\begin{aligned}\frac{dx(t)}{dt}&=h(x(t),\mathbf{y}(t))+g[x_D-x(t)]\ ,\\ \frac{d\mathbf{y}(t)}{dt}&=\mathbf{S}(x(t),\mathbf{y}(t))\ ,\end{aligned} \tag{23}$$

will stabilize the unstable fixed point x_D of (22) in some range of g. For example, when $g\to\infty$, variable x becomes fixed ($x\to x_D$), and the Lyapunov spectrum approaches $\{\lambda_1,\ldots,\lambda_{d-1},-g\}$ where λ_a are conditional Lyapunov exponents of the stable subsystem $\mathbf{y}$, which are all negative by definition.

To provide self-adjustment and tracking of this unstable fixed point we add an equation for x_D in the form

$$\frac{dx_D(t)}{dt}=\mu K[x(t)-x_D(t)]\ . \tag{24}$$

Here again $\mu\ll 1$ is small, and the matrix $\mathbf{g}$ now reduces to a constant $\mathbf{K}=\pm 1$.

The notation may be somewhat confusing here and earlier. We speak of x_D both as a fixed point, thus independent of time, and as slowly varying in time. The idea is that the original dynamics on its own time scale has fixed points independent of time on that "fast" time scale. However, there are drifts in the system which operate on a time scale of order μ^{-1}, and it is on that long time scale that x_D acquires time dependence. The tracking method discussed throughout this paper focuses on capturing and controlling the slow time scale.

The surface of slow motions is now a line

$$x_D=x-\frac{1}{g}h(x,\mathbf{H}(x))\ , \tag{25}$$

where $\mathbf{y}=\mathbf{H}(x)$ is a solution of

$$\mathbf{S}(x,\mathbf{y})=0\ . \tag{26}$$

$\mathbf{H}(x)$ can be multivalued, and all branches have to be considered. For large enough g this line is an attractor for fast motions, although for smaller g this may be not the case. See the next section for an example. Fixed points x^* of the original system (22) lie on the intersection of (25) and the line $x-x_D=0$. The stability of the x^* with respect to slow motions is determined by the structure of the Jacobian and the sign of K. Indeed, linearizing as before near a fixed point $x=x_D=x^*$ yields

$$\begin{aligned}\frac{dx_D(t)}{dt}=\frac{\mu K}{g}&\{[1-g^{-1}h_x(x^*,\mathbf{H}(x^*))]^{-1}-1\}\\&\times[x_D(t)-x^*]\ .\end{aligned} \tag{27}$$

Thus, if $h_x(x^*,\mathbf{H}(x^*))$ is positive, one needs $K=1$ to assure stability of the fixed point x^*, and vice versa. The value of $h_x(x^*,\mathbf{H}(x^*))$ is simply related to the elements of the Jacobian of the original system (1)

$$h_x(x^*,\mathbf{H}(x^*))=DF_{11}+\sum_{i=2}^{d}DF_{1i}DF_{i1}\ . \tag{28}$$

IV. STABILIZATION OF FIXED POINTS IN A CHAOTIC ELECTRIC CIRCUIT

A. Description of the circuit

To demonstrate our method in an experiment we built an electronic circuit with chaotic behavior [11]. The block diagram of the circuit is shown in Fig. 1. The chaotic circuit consists of a nonlinear amplifier which

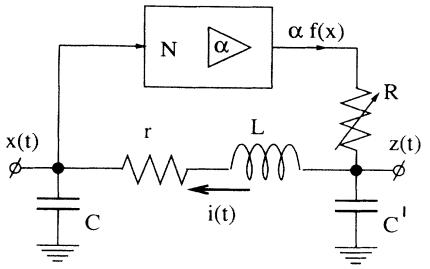

FIG. 1. Block diagram of the chaotic circuit. $R=3.38$ kΩ, $L=145$ mH, $r=347$ Ω, $C=343$ nF, and $C'=225$ nF.

transforms input voltage $x(t)$ into the output $\alpha f(x(t))$. Details of this circuit are found in the paper by Rulkov *et al.* [12]. The output is then applied to the input of the nonlinear amplifier through the low-pass filter RC' and the resonant circuit rLC which can be seen in Fig. 1. The dynamics of the circuit is described by

$$\begin{aligned}\frac{dx(t)}{dt}&=y\ ,\\ \frac{dy(t)}{dt}&=-x-\delta y+z\ ,\\ \frac{dz(t)}{dt}&=\gamma[\alpha f(x)-z]-\sigma y\ .\end{aligned}\tag{29}$$

$x(t)$ is the voltage across the capacitor C and $y(t)=\sqrt{L/C}\,i(t)$ with $i(t)$ the current through the inductor L. $z(t)$ is the voltage across the capacitor C'. Time has been scaled by $1/\sqrt{LC}$.

The parameters of this system have the following dependence on the physical values of the circuit elements:

$$\gamma=\frac{\sqrt{LC}}{RC'},\quad \delta=r\left[\frac{C}{L}\right]^{1/2},\quad \sigma=\frac{C}{C'}\ .\tag{30}$$

The nonlinearity $f(x)$ can be approximated by

$$f(x)\equiv\begin{cases}0.528 & \text{if } x\le -1.2,\\ x(1-x^2) & \text{if } -1.2<x<1.2\\ -0.528 & \text{if } x\ge 1.2.\end{cases}\tag{31}$$

The control parameter α characterizes the gain of the nonlinear amplifier around $x=0$. In the experiments the parameters of the circuit corresponded to the following values for the coefficients in the differential equations (29): $\gamma=0.294$, $\sigma=1.52$, and $\delta=0.534$.

If α is less than 1, all trajectories in the phase space of this system approach the stable fixed point at the origin $x_D=O_0(0,0,0)$. When α becomes larger than unity, the fixed point O_0 is no longer stable, and two additional fixed points $O_L(x_L,0,z_L)$ and $O_R(x_R,0,z_R)$ appear in the phase space of the circuit. The coordinates of these fixed points are given by

$$x_R=z_R=-x_L=-z_L\equiv\sqrt{(\alpha-1)/\alpha}\ .$$

The fixed points O_L and O_R are globally stable in the parameter region

$$1<\alpha<\alpha_H\equiv 1+\frac{(\delta+\gamma)(1+\sigma+\delta\gamma)}{2\gamma}\ .$$

The transition through the critical value α_H is accompanied by a supercritical Andronov-Hopf bifurcation from the fixed points O_L and O_R. The bifurcation gives rise to stable limit cycles P_L and P_R. Note that due to the symmetry of the system any asymmetric limit set coexists with another one which is topologically similar. These can be realized through the transformation $x\to -x, y\to -y, z\to -z$.

For larger values of α the dynamics of the circuit has been explored both experimentally [11] and in numerical simulations [12]. For small enough values of γ, when α increases, a period doubling bifurcation sequence from P_L and P_R leads to the appearance of two chaotic attractors SA_L and SA_R. Then SA_L and SA_R merge into a single symmetric strange attractor SA when α is higher than some critical value. Figure 2 shows the projections of SA_L, SA_R, and SA onto the x-z plane as measured in the experiment.

B. Experimental dynamics of dissipative feedback control

In order to alter the chaotic dynamics of the circuit by controlling the state of the circuit in the vicinity of an unstable fixed point, we introduce the dissipative feedback by applying the external voltage $v(t)$ (see Fig. 3). The idea of dissipative coupling was considered earlier by one of us (N.F.R.) [12–14] for the purpose of synchronizing two chaotic oscillators.

The dynamics of the circuit with the driving is described by

$$\begin{aligned}\frac{dx(t)}{dt}&=y(t)-g[x(t)-v(t)]\ ,\\ \frac{dy(t)}{dt}&=-x(t)-\delta y(t)+z(t)\ ,\\ \frac{dz(t)}{dt}&=\gamma[\alpha f(x(t))-z(t)]-\sigma y(t)\ ,\end{aligned}\tag{32}$$

where $g=(1/R_{\text{coupl}})\sqrt{L/C}$ is the parameter of dissipative coupling of the circuit with the voltage $v(t)$.

We begin by controlling the circuit near the unstable stationary state O_R when $\alpha>\alpha_H$. In this case we apply $v=x_R$ which is the voltage x at the unstable fixed point. This is what we called x_D in our general discussion above. The influence of the driving voltage does not change the coordinates of the fixed point O_R. The strength of the coupling which is needed for the stabilization of the stationary state O_R of the system (32) can easily be found analytically by means of the Routh-Hurwitz criteria, and this is given by

$$g_{\text{cr}}=\frac{-[(\delta+\gamma)^2+1]+\sqrt{[(\delta+\gamma)^2+1]^2+8\gamma(\delta+\gamma)(\alpha-\alpha_H)}}{2(\delta+\gamma)}\ .\tag{33}$$

Local stability of the fixed point O_R is achieved by choosing $g > g_{cr}$. At g_{cr} the fixed point O_R loses stability via a supercritical Hopf bifurcation. Using the Lyapunov function

$$V = \tfrac{1}{2}[(x - x_R)^2 + y^2 + (z - x_R)^2]$$

the global stability of the fixed point (32) follows, if

$$g > \frac{\gamma(0.528\alpha - x_R)^2}{4\sigma(1.2 - x_R)^2} .$$

Due to the symmetry of the system (29), the stability conditions of the fixed point O_L with the dissipative driving $v = x_L$ are the same as for O_R.

When the state of the system approaches the fixed point O_R, the current $I_{coupl} = R_{coupl}[x(t) - v]$ through the resistor R_{coupl} goes to zero. Figure 4 shows the experimentally measured time series of $x(t)$, $z(t)$, and $I_{coupl}(t)$ during the transition from chaotic oscillations of the uncontrolled circuit, corresponding to $R_{coupl} = \infty$ and SW1 switched off, to motion at the stable fixed point O_R achieved with the dissipative coupling turned on and $R_{coupl} = 650\ \Omega$.

For local stabilization of the fixed point $O_0 = (0,0,0)$ with the dissipative driving $v = 0$, the value of the coupling parameter should be chosen in the region

$$g > g_{cr0} = \frac{\gamma(\alpha - 1)}{\sigma + \delta\gamma} . \tag{34}$$

At $g = g_{cr0}$ the fixed point O_0 loses stability and two addi-

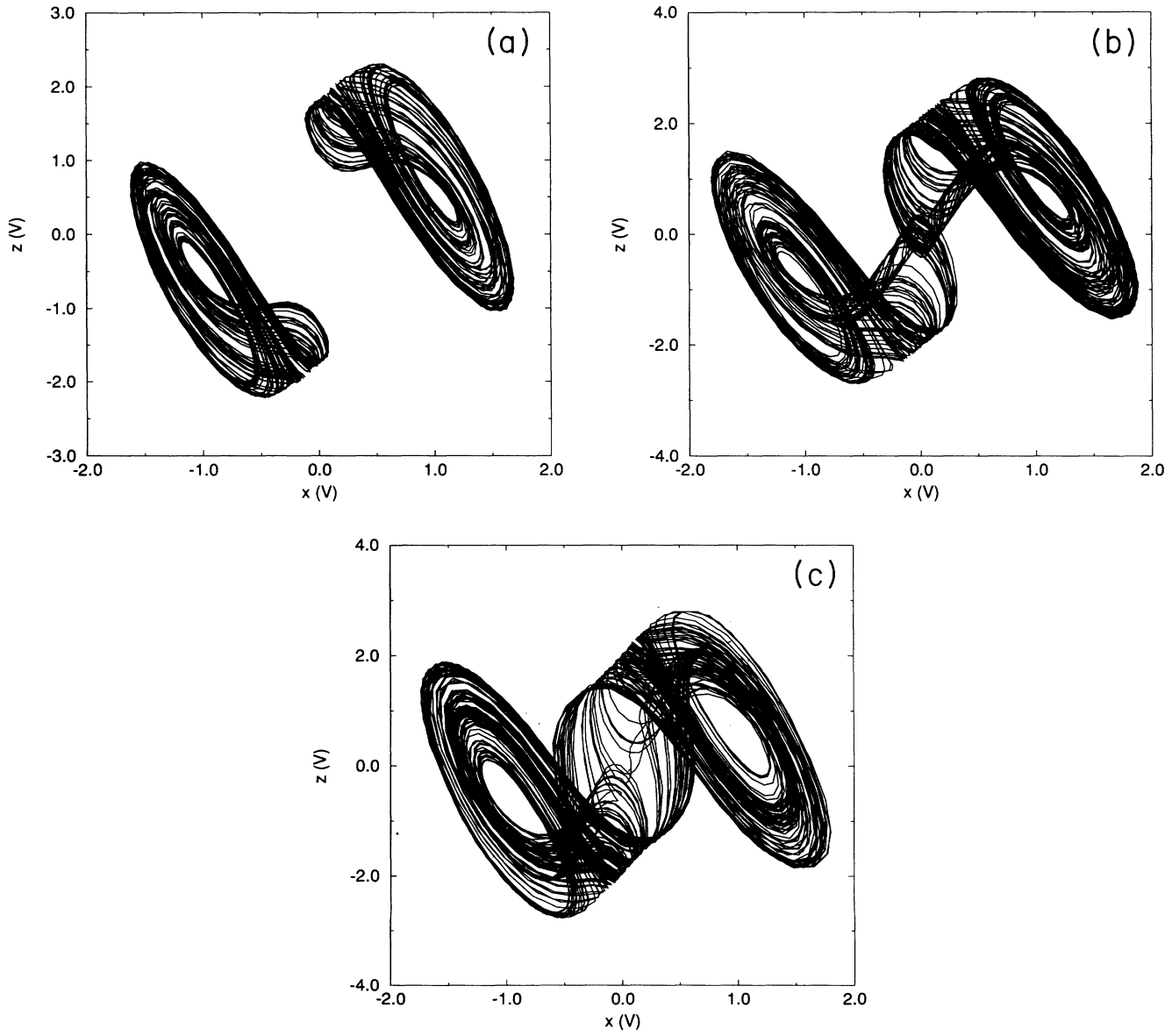

FIG. 2. Chaotic attractors generated by the circuit. The time series $x(t)$ and $z(t)$ are measured with the sampling period $\tau_s = 40$ μsec and plotted in the (x,z) plane. (a) SA_R and SA_L generated with $\alpha = 15.6$. (b) SA with $\alpha = 17.9$. (c) SA with $\alpha = 21.1$.

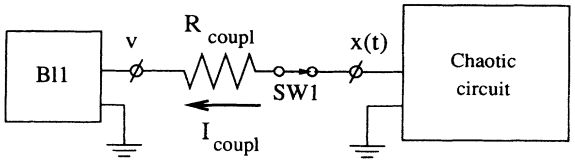

FIG. 3. Block diagram of the experiment with dissipative feedback driving. The voltage v is generated by stabilized source B11. SW1 is a switch.

tional stable fixed points appear as a result of a pitchfork bifurcation. Using the Lyapunov function $V=\frac{1}{2}[x^2+y^2+z^2]$ one can again prove global stability of O_0 when $g>\alpha^2\gamma/4\sigma$.

Experimentally measured time series of $x(t)$,$z(t)$, and I_{coupl} during the transition from chaotic oscillation with $R_{\text{coupl}}=\infty$ to the fixed point O_0 stabilized with $R_{\text{coupl}}=190\ \Omega$ are shown in Fig. 5.

Figure 6 shows the dynamics of the circuit with dissipative feedback control in the experiment with different regimes of driving. When the driving is switched off, the time series $x(t)$ and $z(t)$ clearly display intervals of chaotic oscillations. When the driving is switched on, the pulses of the current I_{coupl} mark the transition to the desired fixed point.

The results of experimental studies of the stability of the fixed points are shown in Fig. 7(a). The boundaries of stability are presented on the parameter plane of coupling g and the slope of the nonlinear function

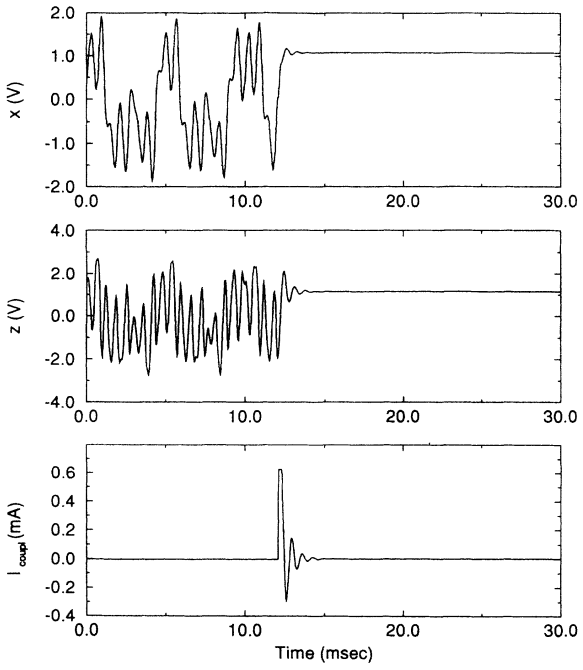

FIG. 4. Time series $x(t)$, $z(t)$, and $I_{\text{coupl}}(t)$ during the transition to O_R after switching on SW1 at time $t_{\text{start}}=12.2$ msec. $\alpha=21.1$, $g=1$, and $\tau_s=40\ \mu$sec.

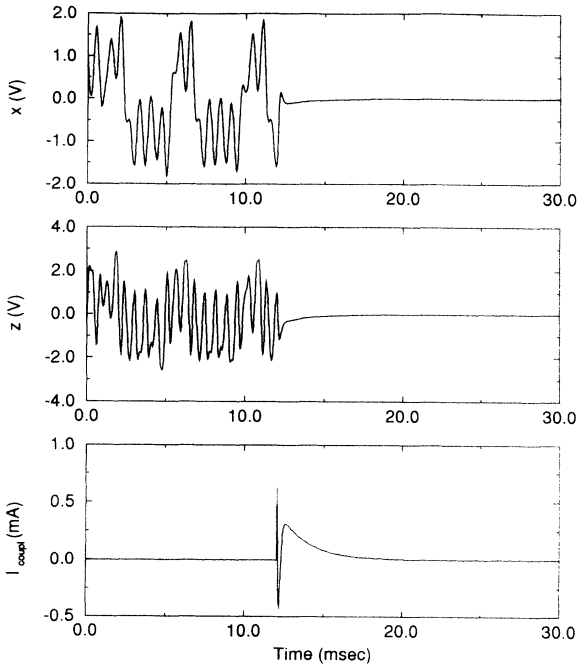

FIG. 5. Time series $x(t)$, $z(t)$, and $I_{\text{coupl}}(t)$ during the transition to O_0 after switching on SW1 at the time $t_{\text{start}}=12.2$ msec. $\alpha=21.1$, $g=3.9$, and $\tau_s=40\ \mu$sec.

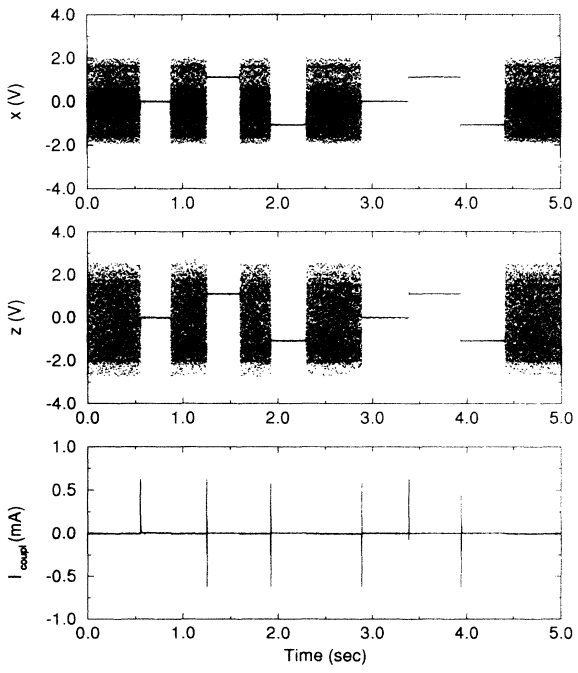

FIG. 6. Time series $x(t)$, $z(t)$, and $I_{\text{coupl}}(t)$ demonstrating the switching of the circuit from chaotic oscillations generated without dissipative feedback control to a controlled fixed point stabilized by the dissipative feedback control v. $\alpha=21.1$, $g=3.42$, and $\tau_s=100\ \mu$sec.

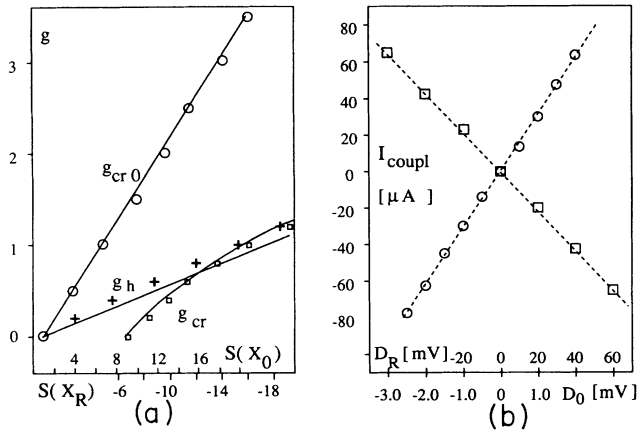

FIG. 7. (a) The stability boundaries g_{cr} and g_{cr0} and the line of heteroclinicity g_h in the (α,g) plane. $\alpha=S(x_0),S(x_R)$ is the slope of nonlinear function $\alpha f(x)$ at the fixed point x_R measured from the circuit. The theoretical boundaries are shown by solid lines. (b) I_{coupl} versus the detuning of the driving v from the coordinate x of the fixed point measured in the experiment with $\alpha=17.9$. Circles show I_{coupl} versus $D_0=(v-x_0)$ with $g=3.42$; squares show I_{coupl} versus $D_R=(v-x_R)$ with $g=1$.

$S(x_i)=\alpha df(x)/dx|_{x=x_i}$ at the fixed point O_i. In the model of the circuit with the nonlinearity given by the expression (31) the slopes have the values $S(0)=\alpha$ and $S(x_R)=3-2\alpha$. Figure 7(b) shows the dependence of the current I_{coupl} on the detuning of the voltage v from the value x_R used in the feedback control of O_R and from the value x_0 used for O_0. It follows from the experimental data presented in Figs. 4–7 that in the regime where the fixed points are stabilized with proper coupling strength, the current through the resistor R_{coupl} goes to zero when the external voltage v is adjusted to the value of the internal voltage x corresponding to the fixed point. This demonstrates that fixed points of a chaotic system may be controlled with small applied external perturbations. Strong driving of the system may be required initially but only during the transition to the region of the fixed point immediately after switching on the control. In order to reduce high current through the resistor R_{coupl} at the beginning of control, one may choose to switch on the coupling at a time when the chaotic trajectory of the circuit comes close to the desired fixed point.

C. Dynamics of control with parameter tracking

To minimize I_{coupl} during the transition period one can start the control of the system with the circuit parameters set to correspond to stability of the desired fixed point. Then one moves the circuit parameters into the region of chaotic dynamics, meanwhile controlling the system near this now unstable fixed point. This procedure is called *tracking* in the literature [8,15]. For the case of dissipative feedback control the value of the stabilizing voltage v has to follow the change of position of the fixed point as the parameters change. In order to adjust the voltage v in the experiment we added to our circuit a self-adjusting feedback. The block diagram of this experiment is shown in Fig. 8. This feedback changes the voltage v as discussed above,

$$\frac{dv(t)}{dt}=\mu K[x(t)-v(t)] , \tag{35}$$

where $\mu\sqrt{LC}/\tau$ and τ is given by the internal characteristics of the integrator Bl2. In the experiment we use $\mu=0.015$. The parameter K is controlled by the switch SW2; $K=+1$ when SW2 is in the position $+$ and $K=-1$ when SW2 is in the position $-$. In this case the feedback matrix $\mathbf{g}$ of Sec. II is simply a scalar K. Recall our remarks about v being both time independent on the fast time scale of the circuit and time dependent on the slow time scale of this tracking feedback.

Consider now the dynamics of the chaotic circuit (32) with the feedback control (35) at $\mu\ll 1$. In this case motion in the four-dimensional phase space has both fast and slow features. The slow motions are located in vicinity of the manifold W_{slow} given by

$$\begin{aligned} &y-g(x-v)=0 , \\ &-x-\delta y+z=0 , \\ &\gamma[\alpha f(x)-z]-\sigma y=0 . \end{aligned} \tag{36}$$

The projection of this one-dimensional manifold W_{slow} onto the (x,v) plane is

$$v=x-\frac{\gamma}{(\sigma+\delta\gamma)}[\alpha f(x)-x] . \tag{37}$$

The direction of motion along the manifold can easily be found from (35). Fast motions of the system are located near the three-dimensional hyperplanes $v=$const and are described by (32). Figure 9 shows qualitatively the slow and fast motions of the system in projection on the plane (x,v). The intersections of the manifold and the three-dimensional hyperplane $v=x$ correspond to the fixed points of the system (32), (35). The projections of these fixed points onto (x,y,z) are the fixed points of the system (29).

It is easy to see from Figs. 9(a) and 9(b) that the fixed points O_R and O_L are attractors with $K>0$ and $g>g_{cr}$

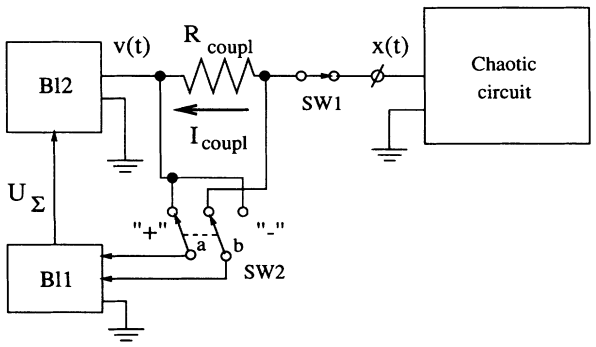

FIG. 8. Block diagram of the experiment with self-adjusting driving v. Bl1 is a subtractor which produces the output $U_\Sigma=a-b$. Bl2 is an integrator.

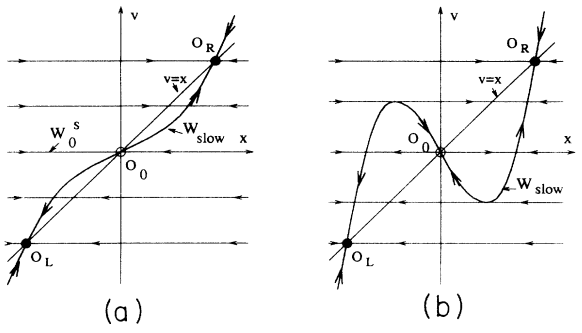

FIG. 9. Manifolds of fast and slow motions in projection onto the (x,v) plane with $K=+1$. (a) $g>g_{cr0}$. (b) $g<g_{cr0}$.

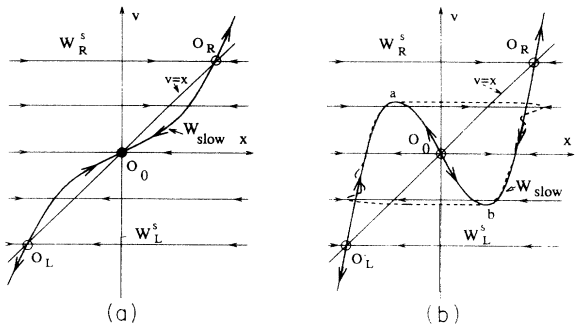

FIG. 11. Manifolds of fast and slow motions in the projection onto the (x,v) plane with $K=-1$. (a) $g>g_{cr0}$. The basin of attraction for the stable fixed point O_0 is bounded by the stable manifolds W^S_R and W^S_L of the fixed points O_R and O_L. (b) $g<g_{cr0}$. The limit cycle P_0 is shown by a dashed line.

as in (33). Depending on initial conditions the system will go to O_R or to O_L. The basins of attraction of the fixed points are separated by the stable manifold W^s_0 of the unstable fixed pointO_0. At the point $g=g_{cr}$ the fixed points lose stability via a supercritical Hopf bifurcation, and two stable limit cycles appear in the three-dimensional hyperplane of fast motions.

Figure 10 presents the observed time series of $x(t)$ and I_{coupl} which show the process of self-adjusting measured in the experiment where the parameter α switches between two values. In this experiment the coordinates of the controlled fixed point O_R change along with the value of α.

The fixed point O_0 with $S(0)>1$ can be an attractor of the system only if $K<0$ and $g>g_{cr0}$ [see Fig. 11(a)]. The basin of the fixed point is restricted by the three-dimensional hyperplanes W^S_R and W^S_L. If $g>g_{cr}$, the hyperplanes are the stable manifolds of the unstable fixed points O_R and O_L. When the parameter g becomes less than g_{cr0}, the fixed point O_0 loses stability and gives rise to the limit cycle P_0 as seen in Fig. 11(b). When g crosses the value g_h, the limit cycle transforms into a heteroclinic loop formed by the stable and unstable manifolds of the

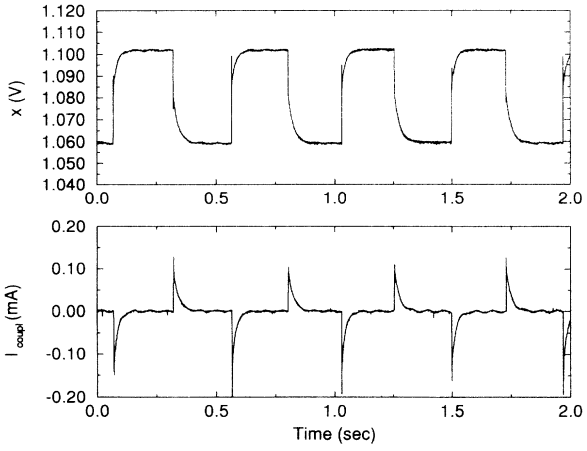

FIG. 10. Time series of $x(t)$ and $I_{coupl}(t)$ in an experiment where α switches between the values 25.4 and 12.9.

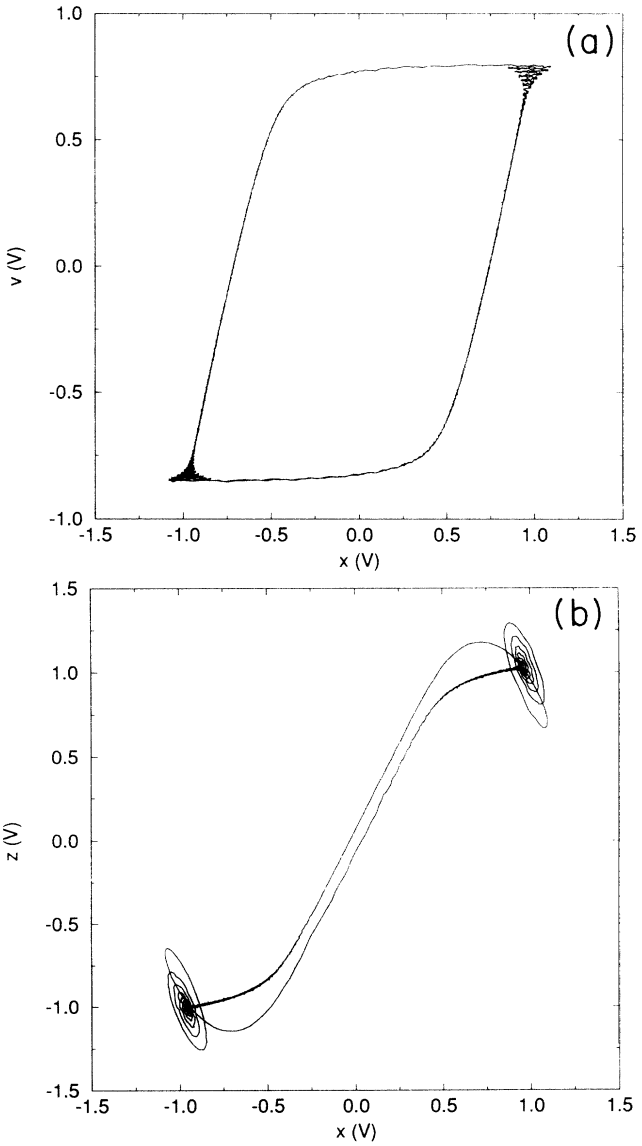

FIG. 12. Limit cycle P_0 measured in the experiment with $\alpha=10.4$, $g=0.6$, and $\tau_s=20$ μsec. (a) Projection onto (x,v). (b) Projection onto (x,z).

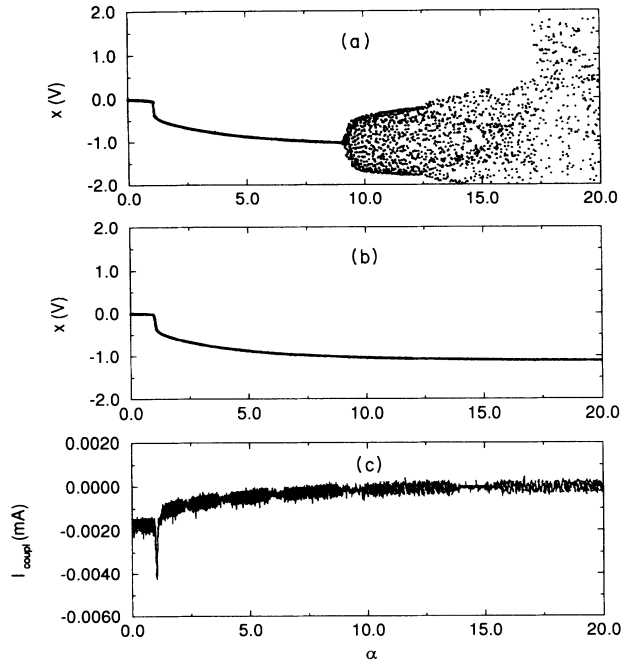

FIG. 13. Experimental data for $x(t)$ and $I_{\text{coupl}}(t)$ verses α. (a) $x(t)$ without control, (b) $x(t)$ with the self-adjusting dissipative control ($K=+1$), and (c) $I_{\text{coupl}}(t)$ measured during the tracking.

fixed points O_R and O_L. In the model equations this happens when the maximum of W_{slow} touches the manifold W_R^S or the minimum of W_{slow} touches W_R^S. This is seen in Fig. 11(b). Using the approximate nonlinear function $f(x)$ one finds that $g_h = g_{\text{cr0}}/4$. The values of the parameters (α, g) corresponding to the heteroclinic loop in the system phase space (32), (36) located at the curve marked by g_h are seen in Fig. 7(a). The crosses in Fig. 7(a) show the parameter values corresponding to the heteroclinicity found in the experiment. Two experimentally measured projections of the limit cycle P_0 onto the planes (x,z) and (x,v) with the parameters of the circuit taken to be close to the heteroclinicity are shown in Figs. 12(a) and 12(b).

To demonstrate the tracking of a fixed point in the experiment we slowly varied the parameter α. One can see from Fig. 13(a) that without control the circuit has a stable fixed point O_L only in the parameter region $\alpha < 8.6$. Using the self-adjusting control with $g=2$ provides stabilization of O_R in the whole range of variation of the parameter α. This is shown in Fig. 13(b). During tracking the values of the current I_{coupl} stayed within the interval $|I_{\text{coupl}}| < 4.5\ \mu\text{A}$ as seen in the time series of Fig. 13(c). In the regime of chaotic oscillations the current through the inductor L can approach values up to 1.2 mA, so the control current remains at most 0.5% of the level of the currents flowing in the circuit.

V. CONCLUSIONS

In this paper we have discussed a general formulation of a method for tracking and stabilizing unstable fixed points and unstable periodic orbits of a chaotic system. The general idea is to add to the system dynamics a feedback which dissipates the dynamical variables toward a desired state $x_D(t)$—the unstable fixed point or the unstable periodic orbit— *and at the same time* to add a "slow" dynamics for the unstable orbit to allow for its drift as parameters of the system slowly vary. We described in detail how to achieve this mixed slow and fast dynamics for fixed points, initially unstable and then stabilized, for a differential equation

$$\frac{d\mathbf{x}(t)}{dt} = \mathbf{F}(\mathbf{x}(t)) , \tag{38}$$

of quite general form. Then we discussed how to stabilize a limit cycle through the same operations used to stabilize fixed points by looking at the sequence of intersections of the limit cycle with Poincaré sections where its appearance is that of a fixed point. The only change required was to cast the operation in terms of a discrete time map on the Poincaré section rather than as a continuous time flow of the original equation.

The idea was demonstrated in detail using a nonlinear circuit which had been extensively studied earlier for other purposes. Both the stabilization of a fixed point and then the stabilization and tracking of the fixed point were shown in this circuit.

The method we have described here is in some sense both less powerful and more practical than the parameter variation technique of Ott, Grebogi, and Yorke [1]. To use that method one must be able to manipulate a parameter of the original system through external forcing. Often one cannot do this either easily or at all. The example noted in the Introduction of controlling a turbulent fluid flow near a wall by varying pressure at the wall serves to illustrate this. The only "parameters" one could vary in such a problem would be the viscosity of the fluid, presumably by heating or cooling the fluid upstream of where one wants to apply control, or possibly by controlling the mean flow by some means unclear to us. Control of pressure at the wall is both feasible and within the scope of the methods discussed here.

The parameter variation technique works best when the region of phase space where the control is to be applied is "targeted" by initial action on the orbit; then the changes in parameter required to maintain the orbit near the previously unstable fixed point or periodic orbit are small because the method takes advantage of the exponentially rapid movement of orbits along the stable manifold of the unstable orbit to which one controls. In the present method basically the same phenomenon allows small external forces to control the system once we have approached the region of the desired state $\mathbf{x}_D(t)$. We do not yet have a way to "target" these states using external forcing. However, once we have arrived at the desired region of phase space, we can remain there even as the system drifts slowly using our tracking methods.

ACKNOWLEDGMENTS

The support of the U.S. Department of Energy Contract No. DE-FG03-90ER14138, ARPA Contract No. 92-F141900-000, and of the Office of Naval Research Contract No. N00014-D-0142 DO #15 is gratefully acknowledged.

[1] E. Ott, C. Grebogi, and J. Yorke, Phys. Rev. Lett. **64**, 1196 (1990).
[2] R. Lima and M. Pettini, Phys. Rev. A **41**, 726 (1990).
[3] E. R. Hunt, Phys. Rev. Lett. **67**, 1953 (1991).
[4] K. Pyragas, Phys. Lett. A **170**, 421 (1992).
[5] M. Jamshiḍi and M. Malek-Zavarei, *Linear Control Systems* (Pergamon, Oxford, 1986).
[6] T. C. Newell, P. M. Alsing, A. Gavrielides, and V. Kovanis, Phys. Rev. E **49**, 313 (1994); Phys. Rev. Lett. **72**, 1647 (1994).
[7] H. D. I. Abarbanel, R. Katz, T. Galib, J. Cembrela, and T. Frison, Phys. Rev. **49**, 4003 (1994).
[8] T. L. Carroll, I. Triandaf, I. Schwartz, and L. Pecora, Phys. Rev. A **46**, 6189 (1992); I. B. Schwartz and I. Triandaf, *ibid.* **46**, 7439 (1992).
[9] H. D. I. Abarbanel, R. Brown, J. J. Sidorowich, and Lev Sh. Tsimring, Rev. Mod. Phys. **65**, 1331 (1993).
[10] L. Pecora and T. Carroll, Phys. Rev. Lett. **64**, 821 (1990).
[11] A. R. Volkovskii and N. F. Rulkov, Pis'ma Zh. Tekh. Fiz. **14**, 1508 (1988) [Sov. Tech. Phys. Lett. **14**, 656 (1988)].
[12] N. F. Rulkov, A. R. Volkovskii, A. Rodrigues-Lozano, E. Del Rio, and M. G. Velarde, Int. J. Bifurcation Chaos **2**, 669 (1992).
[13] A. R. Volkovskii and N. F. Rulkov, Pis'ma Zh. Tekh. Fiz. **15**, 5 (1989) [Sov. Tech. Phys. Lett. **15**, 249 (1989)].
[14] N. F. Rulkov and A. R. Volkovskii, in *Chaos in Communications,* edited by Louis M. Pecora, SPIE Proc. Vol. 2038 (SPIE, Bellingham, WA, 1993).
[15] Z. Gills *et al.*, Phys. Rev. Lett. **69**, 3169 (1992).

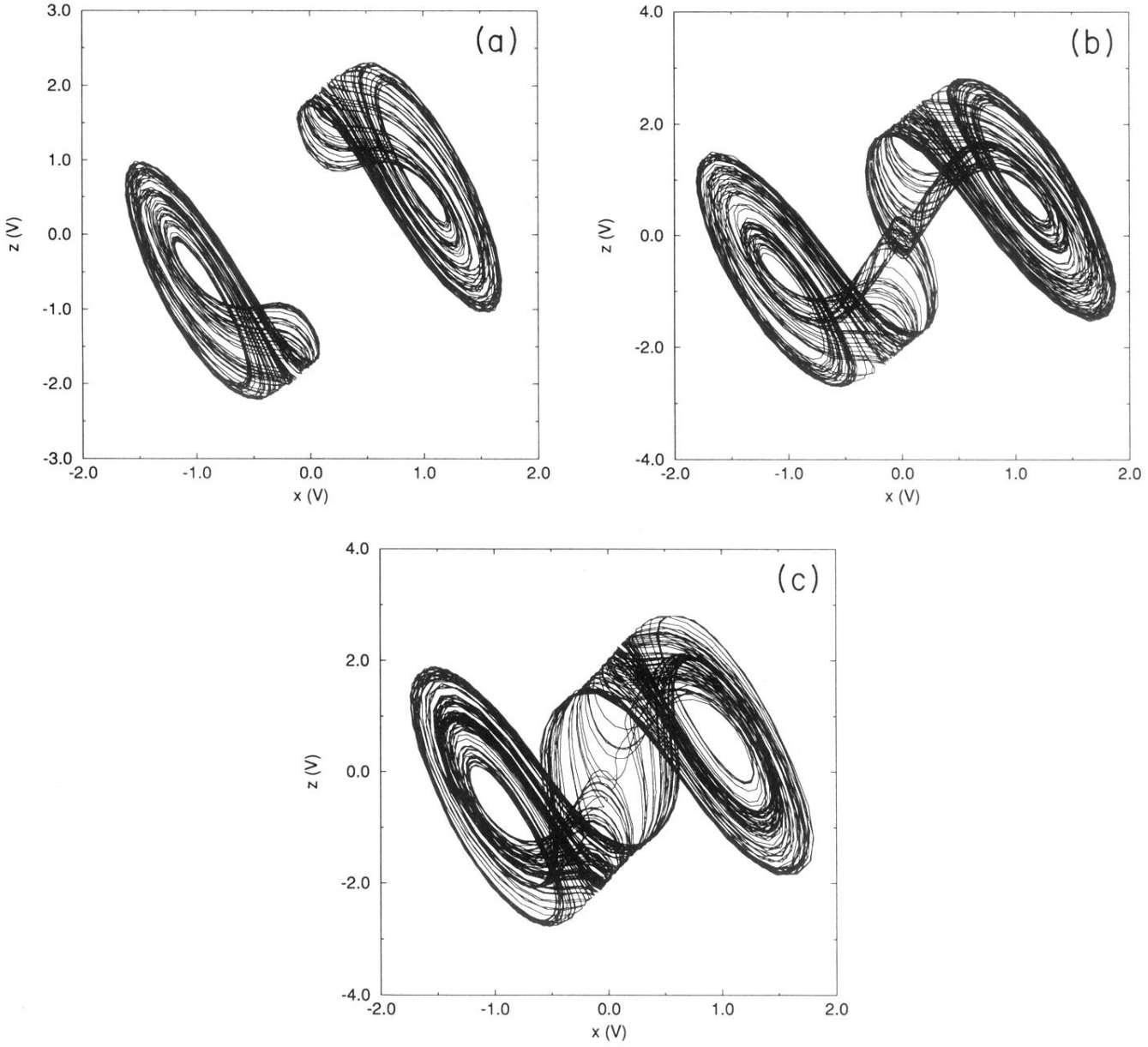

FIG. 2. Chaotic attractors generated by the circuit. The time series $x(t)$ and $z(t)$ are measured with the sampling period $\tau_s = 40$ μsec and plotted in the (x,z) plane. (a) SA_R and SA_L generated with $\alpha = 15.6$. (b) SA with $\alpha = 17.9$. (c) SA with $\alpha = 21.1$.

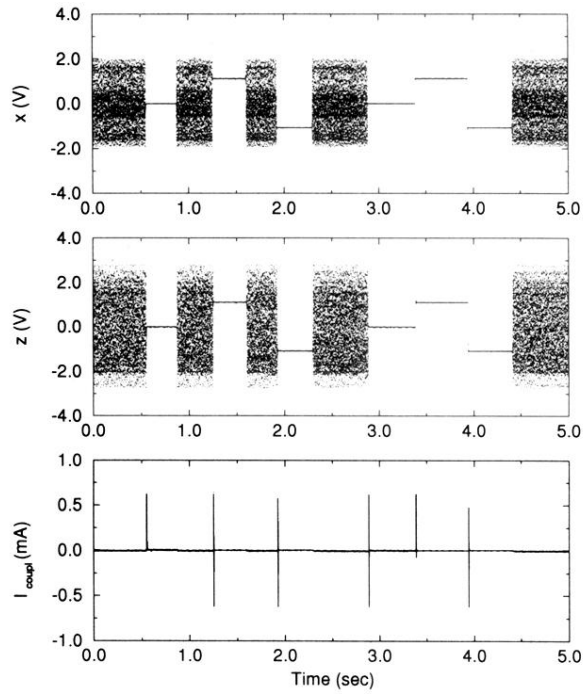

FIG. 6. Time series $x(t)$, $z(t)$, and $I_{\text{coupl}}(t)$ demonstrating the switching of the circuit from chaotic oscillations generated without dissipative feedback control to a controlled fixed point stabilized by the dissipative feedback control v. $\alpha = 21.1$, $g = 3.42$, and $\tau_s = 100\ \mu\text{sec}$.